Demonstration of an erbium-doped fiber with annular doping for low gain compression in cladding-pumped amplifiers

C. Matte-Breton, H. Chen, N. K. Fontaine, R. Ryf, R.-J. Essiambre, C. Kelly, C. Jin, Y. Messaddeq, and S. LaRochelle

OSA Optics Express, (Volume 26, Issue 20) (2018)

https://doi.org/10.1364/OE.26.026633

Demonstration of an erbium-doped fiber with annular doping for low gain compression in cladding-pumped amplifiers

C. MATTE-BRETON,[1] H. CHEN,[2] N. K. FONTAINE,[2] R. RYF,[2] R.-J. ESSIAMBRE,[2] C. KELLY,[3] C. JIN,[1,4] Y. MESSADDEQ,[1] AND SOPHIE LAROCHELLE[1*]

[1]*Centre for Optics, Photonics and Lasers (COPL), Université Laval, Québec, QC, G1V 0A6, Canada*
[2]*Nokia Bell Labs, 791 Holmdel-Keyport Rd, Holmdel, NJ, 07733, USA*
[3]*Nokia Canada, 600 March Rd, Ottawa, ON, K2K 2T6, Canada*
[4]*now with OFS, 19 Schoolhouse Rd, Somerset, NJ, 08873, USA*
**sophie.larochelle@gel.ulaval.ca*

Abstract: We present the design and characterization of a cladding-pumped amplifier with erbium doping located in an annular region near the core. This erbium-doped fiber is proposed to reduce gain saturation, leading to smaller gain compression when compared to uniform core doping. Through numerical simulations, we first compare the performance of three fibers with different erbium doping profiles in the core or the cladding. When the doped fibers are operated at the optimum length, results show that the smaller overlap of the signal mode field with the annular erbium doping region leads to higher gain and lower saturation of the amplifier. A single-core erbium-doped fiber with an annular doping and a D-shaped cladding was fabricated. Measurements demonstrate less than 4 dB of gain compression over the C-band for input power ranging from -40 dBm to 3 dBm. Small gain compression EDFAs are of interest for applications that require input channel reconfiguration. Higher gain and saturation output power are also key issues in cladding-pumped multi-core amplifiers.

OCIS codes: (060.0060) Fiber optics and optical communications; (060.2320) Fiber optics amplifiers and oscillators.

References

1. D. J. Richardson, J. M. Fini, and L. E. Nelson, "Space-division multiplexing in optical fibers," Nat. Photonics **7**, 354-362 (2013).
2. R.-J. Essiambre, G. Kramer, P. J. Winzer, G. J. Foschini, and B. Goebel, "Capacity limits of optical fiber networks," J. Lightwave Technol. **28**, 662-701 (2010).
3. R.-J. Essiambre and R. W. Tkach, "Capacity trends and limits of optical communication networks," Proc. IEEE **100**(5), 1035–1055 (2012).
4. P. J. Winzer, "Scaling optical networking technologies for next generation SDM," in Optical Fiber Communication Conference, San Diego, California, 2018, p. Th1F.4.
5. D. Soma, Y. Wakayama, S. Beppu, S. Sumita, T. Tsuritani, T. Hayashi, T. Nagashima, M. Suzuki, H. Takahashi, K. Igarashi, I. Morita, and M. Suzuki, "10.16-Peta-bit/s dense SDM/WDM transmission over 6-mode 19-core fiber across the C+L Band," J. Lightwave Technol. **36**, 1362-1368 (2018).
6. T. Mizuno, and Y. Miyamoto, "High-capacity dense space division multiplexing transmission," Optical Fiber Technology **35**, 108-117 (2017).
7. K. S. Abedin, J. M. Fini, T. F. Thierry, V. R. Supradeepa, B. Zhu, M. F. Yan, L. Banzal, E. M. Monberg, and D. J. DiGiovanni, "Multicore erbium doped fiber amplifiers for space division multiplexing systems," J. Lightwave Technol. **32**, 2800-2808 (2014).
8. K. S. Abedin, M. F. Yan, T. F. Taunay, B. Zhu, E. M. Monberg, and D. J. DiGiovanni, "State-of-the-art multicore fiber amplifiers for space division multiplexing," Optical Fiber Technology **35**, 64–71 (2017).
9. Y. Sakamaki, T. Kawai, M. Fukutoku, T. Kataoka, and K. Suzuki, "Experimental demonstration of arrayed optical amplifiers with a shared pump laser for realizing colorless, directionless, contentionless ROADM," Opt. Express **20**, B131-B140 (2012).
10. K. S. Abedin, T. F. Taunay, M. Fishteyn, D. J. DiGiovanni, V. R. Supradeepa, J. M. Fini, M. F. Yan, B. Zhu, E. M. Monberg, and F. V. Dimarcello, "Cladding-pumped erbium-doped multicore fiber amplifier," Opt. Express **20**(18), 20191–20200 (2012).

National Science and Engineering Research Council of Canada (NSERC) Funding: RDCPJ 515551-17

11. H. Ono, K. Takenaga, K. Ichii, S. Matsuo, T. Takahashi, H. Masuda, and M. Yamada, "12-core double-clad Er/Yb-doped fiber amplifier employing free-space coupling pump/signal combiner module," in European Conference on Optical Communication (ECOC, 2013), paper We.4.A.4.
12. S. Jain, T. Mizuno, Y. Jung, Q. Kang, J. Hayes, M. Petrovich, G. Bai, and H. Ono, "32-core inline multicore fiber amplifier for dense space division multiplexed transmission system," in European Conference on Optical Communication (ECOC, 2016), paper Th.3.A.1.
13. H. Chen, N. K. Fontaine, R. Ryf, C. Jin, B. Huang, K. Shang, R.-J. Essiambre, L. Wang, T. Hayashi, T. Nagashima, T. Sasaki, Y. Messaddeq, and S. LaRochelle, "Demonstration of cladding-pumped six-core erbium-doped fiber amplifier," J. Lightwave Technol. **34**, 1654-1660 (2016).
14. C. Jin, B. Ung, Y. Messaddeq, and S. LaRochelle, "Annular-cladding erbium doped multicore fiber for SDM amplification," Opt. Express **23**, 29647-29659 (2015).
15. H. Chen, C. Jin, B. Huang, N. K. Fontaine, R. Ryf, K. Shang, N. Grégoire, S. Morency, R.-J. Essiambre, G. Li, Y. Messaddeq, and S. LaRochelle, "Integrated cladding-pumped multicore few-mode erbium-doped fibre amplifier for space-division multiplexed communications," Nat. Photonics **10**(8), 529–533 (2016).
16. M. Wada, T. Sakamoto, S. Aozasa, T. Mori, T. Yamamoto, and K. Nakajima, "Two-LP-mode six-core cladding pumped EDFA with high pump power density," J. Lightwave Technol. **36**, 331-335 (2018).
17. K. Takeshima, T. Tsuritani, Y. Tsuchida, K. Maeda, T. Saito, K. Watanabe, T. Sasa, K. Imamura, R. Sugizaki, K. Igarashi, I. Morita, and M. Suzuki, "51.1-Tbit/s MCF transmission over 2520 km using cladding-pumped seven-core EDFAs," J. Lightwave Technol. **34**, 761-767 (2016).
18. C. Castro, S. Jain, E. D. Man, Y. Jung, J. Hayes, S. Calabrò, K. Pulverer, M. Bohn, S. Alam, D. John Richardson, K. Takenaga, T. Mizuno, Y. Miyamoto, T. Morioka, and W. Rosenkranz, "100-Gb/s transmission over a 2520-km integrated MCF system using cladding-pumped amplifiers," IEEE Photon. Technol. Lett. **29**, 1187-1190 (2017).
19. Z. Várallyay, and J. C. Jasapara, "Comparison of amplification in large area fibers using cladding-pump and fundamental-mode core-pump schemes," Opt. Express **17**(20), 17242-17252 (2009).
20. Q. Kang, E. L. Lim, Y. Jung, J. K. Sahu, F. Poletti, C. Baskiotis, S. U. Alam, and D. J. Richardson, "Accurate modal gain control in a multimode erbium doped fiber amplifier incorporating ring doping and a simple LP01 pump configuration," Opt. Express **20**(19), 20835–20843 (2012).
21. C. Jin, B. Ung, Y. Messaddeq, and S. LaRochelle, "Tailored modal gain in a multi-mode erbium-doped fiber amplifier based on engineered ring doping profiles," Proc. SPIE **8915**, 89150A (2013).
22. Q. Kang, E.-L. Lim, F. P. Y. Jung, C. Baskiotis, S.-u. Alam, and D. J. Richardson, "Minimizing differential modal gain in cladding-pumped EDFAs supporting four and six mode groups," Opt. Express **22**, 21499-21507 (2014).
23. J. Nilsson,J. D. Minelly, R. Paschotta, A. C. Tropper, and D. C. Hanna, "Ring-doped cladding-pumped single-mode three-level fiber laser," Optics letters, **23**(5), 355-357 (1998).
24. P. Bousselet, C. Simonneau, C. Moreau, L. Provost, P. Lambelet, X. Rejeaunier, F. Leplingard, L. Gasca, and D. Bayart, "+33dBm output power from a full C-band cladding diode-pumped EDFA," in European Conference on Optical Communication (ECOC, 2002), paper PD1.7.
25. C. Matte-Breton, H. Chen, N. Fontaine, R. Ryf, R-J. Essiambre, Y. Messaddeq, and S. LaRochelle, "Cladding pumped EDFAs with annular erbium doping," in Conference on Lasers and Electro-Optics (CLEO, 2018), paper JTH2A.133.
26. L. Gagné-Godbout, *Modélisation, fabrication et caractérisation d'un amplificateur à fibre optique à sept cœurs dopés à l'erbium* (Université Laval, 2014), Chap. 4.
27. B. J. Ainslie, "A review of the fabrication and properties of erbium-doped fibers for optical amplifiers," J. Lightwave Technol. **9**(2), 220-227 (1991).
28. H. Zellmer, A. Tünnermann, H. Welling, and V. Reichel, "Double-clad fiber laser with 30 W output power," in Optical Amplifiers and Their Applications (Optical Society of America, 1997), paper FAW18.
29. D. E. McCumber, "Einstein relations connecting broadband emission and absorption spectra," Physical Review **136**(4A), A954. (1964).
30. B. Pedersen, A. Bjarklev, J. H. Povlsen, K. Dybdal, and C. C. Larsen, "The design of erbium-doped fiber amplifiers," J. Lightwave Technol. **9**(9), 1105-1112 (1991).

1. Introduction

Fueled by cloud-based applications, video streaming and supercomputing, data traffic carried by communication networks has grown considerably in the last few decades. Optical fibers are deployed worldwide to form the backbone of high capacity networks that must deliver an ever increasing bandwidth with reduced cost and complexity. In this context, space-division-multiplexing (SDM) is currently being investigated as a possible means to scale optical fiber capacity beyond the fundamental limit of single-mode single-core optical fibers [1-4]. Recent demonstrations of transmissions over few-mode multi-core fibers show that the number of channels could be increased by two orders of magnitude, allowing in excess of 10 Pb/s transmission per optical fiber link [5-6]. A key technology to the deployment of SDM links is

National Science and Engineering Research Council of Canada (NSERC) Funding: RDCPJ 515551-17

a compatible in-line optical fiber amplifier [7-8], which should ideally avoid the demultiplexing of spatial channels often done before amplification in laboratory experiments of SDM transmission. A spatially integrated optical amplifier sharing the same pump is also of interest for applications requiring a compact solution for switching and routing [9].

Although initial work on multi-core erbium-doped fiber amplifiers (MC-EDFAs) used in-core pumping, there is a growing interest in cladding-pumped MC-EDFAs [10-18]. Erbium-doped fiber amplifiers (EDFAs) with in-core pumping are well-known for their high performance in terms of gain, noise, optical bandwidth and power efficiency. However, in multi-core SDM links, these advantages are offset by the need to introduce demultiplexing and multiplexing stages at the amplifier input in order to insert the pump in each core. In-core pumping therefore leads to a high component count while cladding pumping can decrease system complexity and cost by eliminating the need for components such as pump-signal multiplexers. An additional advantage of cladding pumping that is of particular interest is the use of a single high-power pump source that can be side-coupled to the double-clad fiber. In this configuration, a low cost multimode pump can be used as the pump does not need to be coupled to a single-mode fiber to be injected in the amplifier. Another advantage of cladding pumping arises in SDM links with mode-multiplexing. When simultaneously amplifying multiple modes, the more uniform pump power distribution over the optical fiber cross-section can reduce differential modal gain [19]. Numerous cladding-pumped MC-EDFAs have thus been fabricated and characterized with several designs proposing solutions to address the low pumping efficiency. A few examples are a six-core EDFA with more than 20 dB gain over the 1542 nm – 1576 nm wavelength range [10], a 32-core co-doped Er/Yb fiber amplifier with >17 dB gain over the 1544 nm – 1564 nm wavelength range [12] and an EDFA with six cores, each delivering >18 dBm output power with >17 dB gain over the C-band [13]. Few-mode MC-EDFAs were also demonstrated using an annular cladding [14-15] or slightly coupled cores [16] to increase pump intensity and pumping efficiency.

Cladding pumping presents new opportunities for engineering the erbium doping profile in order to improve the amplifier performance. For instance, ring doping, which consists of including erbium ions in an annular region rather than doping the core uniformly, or a structured erbium concentration profile can be used to reduce differential modal gain [20-22] or to increase output power [23-24]. More generally, assuming uniform distribution of the pump in the cladding, annular doping allows to control the signal overlap with the erbium-doped region without modifying the pump overlap. This is illustrated in Fig. 1 that compares the mode intensity profiles of an EDFA with in-core pumping and uniform doping in the core [Fig. 1(a)], to the mode intensity profiles of an EDFA with cladding pumping having an annular-doped region in the core [Fig. 1(b)]. In this particular case, the optical fiber supports two mode groups, LP_{01} and LP_{11}, and the relative gain of the two modes is controlled through the erbium doping profile (see for example [20]). In this work, we consider a double-clad optical fiber with an annular erbium-doped region located in the cladding for amplification of a single mode [Fig. 1(c)]. The purpose of this design is to reduce signal overlap with the doped region in order to reduce saturation and minimize gain compression [23-24], which is an important advantage for EDFAs used in dynamic and reconfigurable networks. To our knowledge this is the first direct detailed comparison of simulation and measurement of a cladding-pumped EDFA, with erbium-ion doping located in the cladding, that is designed specifically to lower gain compression.

National Science and Engineering Research Council of Canada (NSERC) Funding: RDCPJ 515551-17

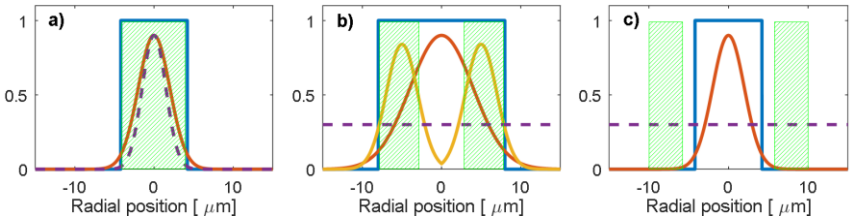

Fig. 1. Normalized LP_{01} (orange) and LP_{11} (yellow) mode intensity profiles, and normalized pump intensity distribution (purple, dashed) of: a) a core-pumped single-mode fiber, b) a cladding-pumped multi-mode fiber with erbium doping in an annular region of the core, and c) a cladding-pumped single-mode fiber with erbium doping in the cladding close to the core. The blue line indicates the refractive index profile and the shaded green area is the erbium-doped region.

In this paper, we expand on our initial report in [25] and present here in detail the optimization of the doped fiber design and compare simulation results to experimental measurements. The paper is focused on optimizing the erbium doping profile to reduce gain compression in a single-mode fiber amplifier. While we investigate the simulation and fabrication of a single-core fiber, the results could be straightforwardly extended to MC-EDFA. In section 2, we simulate different doped fiber designs and compare their minimum gain over the C-band for a maximum of 4 dB of gain compression. The ideal gain compression of an EDFA used in dynamic and reconfigurable network would be 0 dB to avoid gain excursions when channels are rerouted. However, the lower the gain compression, the harder it is to achieve a high minimum gain over a significant input power range. These simulations are performed using standard values found in the literature for erbium-doped alumino-silicate glass. In section 3, we first characterize the parameters of a fabricated fiber with annular-doping in the cladding. We then use a tapered fiber to inject the pump in the cladding and measure the amplifier gain and NF. Using the experimentally determined parameters, we compare simulation results to validate the approach. Finally, we conclude, in section 4, by a discussion and recommendations for further MC-EDFAs designs.

2. Design of the erbium-doped fiber

As optical channels are routed through reconfigurable networks, the input power to an EDFA can vary leading to transients for the remaining channels. A useful measure to quantify the impact of changing the number of input channels is the static gain compression. Gain compression at a given signal wavelength is defined as the gain difference for two values of total input power. Operation of EDFAs in saturation will therefore lead to high gain compression as the gain changes more rapidly with input power when the amplifier input power is above its saturation power. In this paper, we propose to modify the erbium doping profile of a cladding-pumped fiber to investigate how to achieve sufficient gain and output power, while maintaining low gain compression. By placing the erbium ions (Er^{3+}) in the evanescent tail of the signal mode field, i.e. in an annular region located in the cladding but close to the core, the local signal intensity overlapping with the doped region remains low even as the amplifier gain increases. In this section, we compare three fiber designs to illustrate this behavior. We perform numerical simulations using a standard rate equation model with fiber parameters compatible with common fabrication processes such as modified chemical vapor deposition (MCVD) with solution doping. We examine fiber designs meeting a target of <4 dB of gain compression and contrast their minimum achievable gain and fiber length.

National Science and Engineering Research Council of Canada (NSERC) Funding: RDCPJ 515551-17

2.1 Erbium doping profiles

To minimize the number of fabrication steps, we simulate radially dependent erbium doping profiles that have only one erbium ion (Er^{3+}) concentration level, namely ρ_0=1x10^{25} ions/m^3. The three fibers under study are a fiber with uniform doping across the core (Fiber A), a fiber with a uniformly doped annular region in the cladding (Fiber B) and a fiber in which both the core and a portion of the cladding are doped with the same concentration of Er^{3+} (Fiber C). The refractive index profiles and the Er^{3+} concentration profiles of the three fibers are illustrated in Fig. 2. All three fibers have a silica cladding with an index of 1.4440 at 1550 nm. Fiber A is a step-index fiber with core radius of 4.5 µm and refractive index of 1.4502. The numerical aperture is 0.134 and the V number is 2.44 at 1550 nm, which mean that the LP_{11} mode is very close to cutoff. In cladding-pumped amplifiers, enlarging the cores to reduce signal intensity helps to reduce saturation [13]. In Fiber B and C, because some Er^{3+} are incorporated in the cladding, silica is replaced by alumino-silicate to increase the solubility of the Er^{3+} in this region. Therefore, the region between r=4.5 µm and r=9.5 µm has a refractive index of 1.4460, which is a reasonable value for alumino-silicate to accept an Er^{3+} concentration of 1x10^{25} ions/m^3. For Fiber B, the erbium doping is only found between r=6 µm and r=9.5 µm while, for comparison purposes, Fiber C is doped with erbium from r=0 µm to r=9.5 µm.

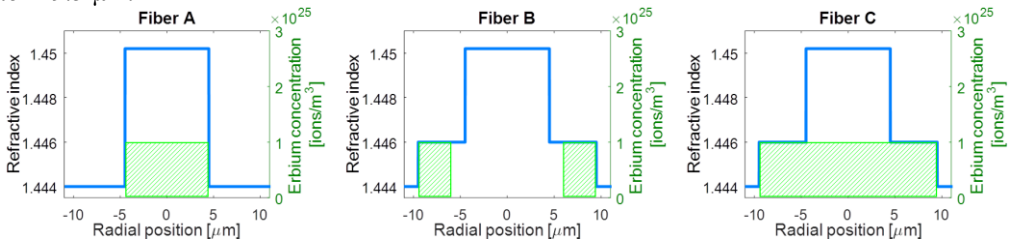

Fig. 2. Refractive index (blue line) and erbium concentration (green shaded area) profiles of fibers A, B and C.

2.2 Model and simulations

Simulations were performed using the standard EDFA two-level model with the usual set of power propagation and population rate equations in which we introduce radial resolution as described in [10]. Since we aim to design single-mode cores, only the LP_{01} mode is considered in the simulations for the signal (we assume that no higher-order modes are present). The pump power is assumed to be uniformly distributed in the cladding that has a diameter of 140 µm. Consequently, there is not azimuthal dependence and we divide the fiber cross-section in K rings, each with uniform Er^{3+} concentration, and we calculate the average inversion of each ring to calculate transition rates and gain. We write

$$\begin{cases} \frac{dP_p(z)}{dz} = -\sigma_{ap}\left(\sum_{k=1}^{K} n_{1,k}(z)\,\Gamma_{p,k}\right)P_p(z) - \alpha_p P_p(z) \\ \frac{dP_{s,\lambda}(z)}{dz} = \left(\sigma_{e,\lambda}\sum_{k=1}^{K} n_{2,k}(z)\,\Gamma_{\lambda,k} - \sigma_{a,\lambda}\sum_{k=1}^{K} n_{1,k}(z)\,\Gamma_{\lambda,k}\right)P_{s,\lambda}(z) - \alpha_s P_{s,\lambda}(z) \\ \frac{dP^{\pm}_{ASE,\lambda}(z)}{dz} = \left(\sigma_{e,\lambda}\sum_{k=1}^{K} n_{2,k}(z)\,\Gamma_{\lambda,k} - \sigma_{a,\lambda}\sum_{k=1}^{K} n_{1,k}(z)\,\Gamma_{\lambda,k}\right)P^{\pm}_{ASE,\lambda}(z) \\ \qquad +\sigma_{e,\lambda}\left(\sum_{k=1}^{K} n_{2,k}(z)\,\Gamma_{\lambda,k}\right)2h\nu_\lambda\Delta\nu_\lambda - \alpha_s P^{\pm}_{ASE,\lambda}(z) \end{cases} \quad (1)$$

$$\begin{cases} n_{1,k}(z) = \frac{\frac{A_k}{\tau}+W_{3,k}(z)}{W_{1,k}(z)+W_{2,k}(z)+W_{3,k}(z)+\frac{A_k}{\tau}}\rho_k(z) \\ n_{2,k}(z) = \frac{W_{1,k}(z)+W_{2,k}(z)}{W_{1,k}(z)+W_{2,k}(z)+W_{3,k}(z)+\frac{A_k}{\tau}}\rho_k(z) \\ \rho_k(z) = n_{1,k}(z) + n_{2,k}(z) \end{cases} \quad (2)$$

National Science and Engineering Research Council of Canada (NSERC) Funding: RDCPJ 515551-17

$$\begin{cases} W_{1,k}(z) = \frac{\sigma_{ap}\Gamma_{p,k}P_p(z)}{h\nu_p} \\ W_{2,k}(z) = \sum_{\lambda,s}\frac{\sigma_{a,\lambda}\Gamma_{\lambda,k}P_{s,\lambda}(z)}{h\nu_\lambda} + \sum_{\lambda,\mathrm{ASE}}\frac{\sigma_{a,\lambda}\Gamma_{\lambda,k}P_{ASE,\lambda}(z)}{h\nu_\lambda} \\ W_{3,k}(z) = \sum_{\lambda,s}\frac{\sigma_{e,\lambda}\Gamma_{\lambda,k}P_{s,\lambda}(z)}{h\nu_\lambda} + \sum_{\lambda,\mathrm{ASE}}\frac{\sigma_{e,\lambda}\Gamma_{\lambda,k}P_{ASE,\lambda}(z)}{h\nu_\lambda} \end{cases} \quad (3)$$

where λ stands for the wavelength channels of the signal or the amplified spontaneous emission (ASE), and k refers to the different rings with area A_k. Eq. (1) describes the propagation of the pump power, P_p, the signal, P_s, and the ASE, $P^{\pm}_{ASE}$, in the forward (+) and backward (-) direction. The pump is co-propagating with the signal and the respective background loss of the pump and the signal are α_p and α_s. Also, σ_{ap} is the absorption cross-section at 980 nm, $\sigma_{e,\lambda}$ and $\sigma_{a,\lambda}$ are the emission and absorption cross-sections at the signal or ASE wavelengths. The pump and signal (or ASE) overlaps with each ring are $\Gamma_{p,k}$, and $\Gamma_{\lambda,k}$ respectively. Eq. (2) describes the radially resolved population inversion along the fiber. The lower and upper population level densities of a given ring are $n_{1,k}$ and $n_{2,k}$, while ρ_k is the erbium concentration of a given doped ring. For the design, ρ_k is either 0 or ρ_0. When simulating experimental results, ρ_k will vary from ring to ring. Eq. (3) represents the transition rates associated with pump absorption (W_1), signal and ASE absorption (W_2), and signal and ASE stimulated emission (W_3). As usual, h is the Planck constant, ν_p and ν_λ are the pump frequency and signal (or ASE) frequency, and τ is the lifetime of the Er^{3+} upper metastable level.

For the simulations, we consider 31 signal channels uniformly distributed over the C-band (1530 nm to 1560 nm) and 201 ASE channels between 1420 nm and 1620 nm. The spectral resolution of the simulations is therefore 1 nm. At first, we neglect background propagation loss (α_s and α_p are set to 0 dB/m). We use absorption and emission cross-sections measured on an erbium-doped alumino-silicate fiber previously fabricated in our laboratory [26], which are illustrated in Fig. 3. The fiber cross-section between radius r=0 to r=10 μm is divided into 100 rings. The signal and ASE confinement for each ring, over the whole spectrum of interest (i.e. 1420 nm to 1620 nm with 1 nm resolution), were found by simulating the LP01 mode profile with COMSOL. Although not necessary for step-index fibers, this numerical technique is useful when considering variations of the index profile in the cladding and necessary when doing the simulations of the experimentally measured profile in section 3 below. The pump overlap for each ring was straightforwardly found by considering that the pump power is uniformly distributed over the fiber cross-section.

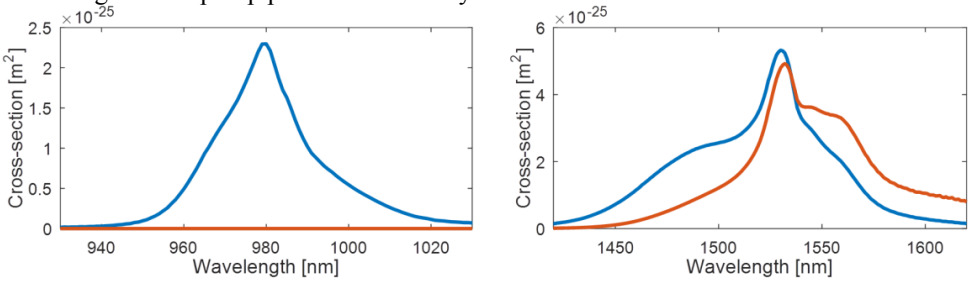

Fig. 3. Absorption (blue) and emission (orange) cross-sections used in simulations (from [25]).

Our target is to achieve a maximum of 4 dB of gain compression over the C-band when the total input power is varied from -40 dBm (unsaturated amplifier) to 3 dBm (fully loaded amplifier). This total input power is uniformly distributed over the 31 channels. Considering that 3 dBm corresponds to a fully loaded amplifier (all 31 channels present at its input), the calculated gain compression represents a worst case scenario. If a sub-band is absent from the EDFA input, the amplifier will be less saturated and the gain compression will be lower for

National Science and Engineering Research Council of Canada (NSERC) Funding: RDCPJ 515551-17

the remaining channels, whatever the specific wavelengths of the sub-band channels that are absent. The simulations parameters are summarized in Table 1 where $P_{p,in}$ is the input pump power, $P_{s,in,unsat}$ and $P_{s,in,sat}$ are the limits of the total input signal power range used to calculate the gain compression, r_{clad} is the radius of the cladding, n_{core} is the refractive index of the core, n_{doped} is the refractive index of the erbium-doped alumino-silicate region around the core, n_{clad} is the refractive index of the cladding.

Table 1. Parameters used in initial simulations, common to all fibers.

Parameter	Value	Unit
$P_{p,in}$	14.5	W
ρ	1×10^{25}	ions/m^3
$P_{s,in,sat}$	3 (-11.91 dBm/ch)	dBm
$P_{s,in,unsat}$	-40 (-54.91 dBm/ch)	dBm
σ_{ap}	2.297×10^{-25}	m^{-2}
α_p	0	m^{-1}
α_s	0	m^{-1}
r_{clad}	70	µm
n_{core}	1.4502	-
n_{doped}	1.4460	-
n_{clad}	1.4440	-

For each fiber, we simulated different lengths in order to maximize the minimum gain over the C-band with less than 4 dB of gain compression over the total input power range. The resulting lengths were 0.87 m, 18.2 m and 0.84 m respectively for fibers A, B and C. Fig. 4 shows the spectral gain of each fiber calculated with these lengths for the minimum and maximum total input signal power. For each fiber, the maximum gain compression (4 dB) occurs around 1532 nm. The minimum gain, among the 31 channels, for an input power of 3 dBm for fibers A, B and C was respectively 6.8 dB, 17.7 dB and 8.1 dB. With the optimized length, the saturated output power is found by calculating the total signal output power at the 3-dB saturation point of the average amplifier gain. For fibers A, B and C, we find respectively 10.7 dBm, 22.3 dBm and 12.1 dBm. Thus, according to the simulations, Fiber B, with the Er^{3+} located in an annular region of the cladding, is far superior in terms of minimum gain when limiting the gain compression to 4 dB.

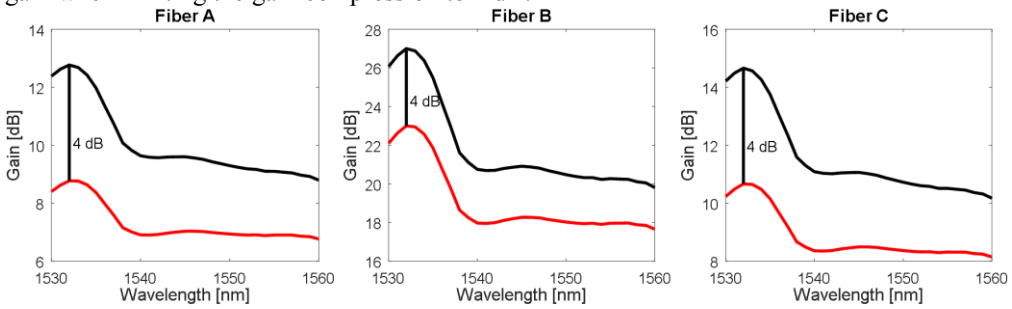

Fig. 4. Gain as a function of wavelength for total input power of -40 dBm (black) and 3 dBm (red) distributed over 31 channels at the optimum length for each fiber.

3. Fiber fabrication and characterization

In order to validate the approach, we fabricated Fiber B using MCVD and solution doping technique. We first deposited a layer of silica sooth using the solution doping technique with

National Science and Engineering Research Council of Canada (NSERC) Funding: RDCPJ 515551-17

Al_2O_3 and Er_2O_3 to dissolve the Er^{3+} ions in the porous glass [27]. This layer corresponds to the region r=6.0–9.5 μm of the design. This was followed by a second step of MCVD deposition for the fiber core that was made of GeO_2 doped SiO_2 since there was no Er^{3+} doping in this region. Firstly a buffer layer was deposited between r=4.5–6.0 μm with a GeO_2 concentration to match the index of the alumino-silicate glass, then the GeO_2 concentration is increased for the core. In order to break the symmetry of higher-order pump modes, a flat surface was polished on the preform resulting in an optical fiber having a "D"-shaped cross-section [28]. The fiber diameter was 140 μm and a low-index (1.37) polymer with a 205 μm diameter was used to confine the pump power in the cladding.

3.1 Fiber parameters measurements

We measured the resulting refractive index profile of the fiber, at the center of the preform, using a refracted near-field analyzer (Exfo NR-9200HR) at 657.6 nm. The measured refractive profile, neglecting dispersion of the refractive index step, was scaled down to the fiber dimension to compare it to the design in Fig. 5(a). We imported this profile into COMSOL in order to calculate the LP_{01} mode confinement in each ring more accurately in subsequent numerical simulations of experimental measurements. The COMSOL simulations also indicated that, although close to cut-off, the LP_{11} mode is guided (at 1530 nm, $n_{eff,LP01}=n_{clad}+ 25.0\text{x}10^{-4}$, $n_{eff,LP11}=n_{clad}+4.67\text{x}10^{-4}$). Fig. 6 shows the signal overlap in each ring calculated from the measured refractive index profile and compares the result to the ones of the design at 1550 nm. The fabricated fiber has 53% more signal overlap than the designed one in the 6 μm < r < 9.5 μm region (Γ = 0.1345 compared to Γ = 0.0877). Using the signal overlap that was calculated from this measurement, numerical simulations were repeated with all other parameters corresponding to the design ones. This leads to an optimal fiber length of 11.1 m and a minimum gain of 16.5 dB for 4 dB of gain compression.

The erbium concentration was measured on the preform as a function of the radial position, using an electron micro-probe analyzer (CAMECA) with a measurement sensitivity of $\Delta\rho=5\text{x}10^{24}$ ions/m^3 , which is close to the doping level of the fiber thereby resulting in a noisy measurement. We performed a fit using a half-Lambertian (r<7.4μm) and half-Gaussian (r>7.4μm) profile and used it for the simulations. The asymmetry of this fit allow to consider, in the simulations, the small amount of erbium that was measured above the detection threshold of the CAMECA ($2\text{x}10^{24}$ ions/m^3) in the r < 6 μm region. Note that the electron micro-probe analysis showed that a small amount of germanium was present in the erbium-doped region. Both the measured and fitted erbium concentration profiles are compared to the design in Fig. 5(b). Note that the obtained erbium ion content is significantly lower than the design with an average concentration of $\rho=3.7\text{x}10^{24}$ ions/m^3 in the 6 μm < r < 9.5 μm region. Using this averaged concentration in all the doped rings, numerical simulations results in an optimal length of 49.1 m and a minimum gain of 17.6 dB. Using the measured erbium concentration profile directly in the initial simulations leads to an optimal fiber length of 25.5 m and a minimum gain of 14.2 dB. In both cases, all other parameters correspond to the design ones, including the overlap.

National Science and Engineering Research Council of Canada (NSERC) Funding: RDCPJ 515551-17

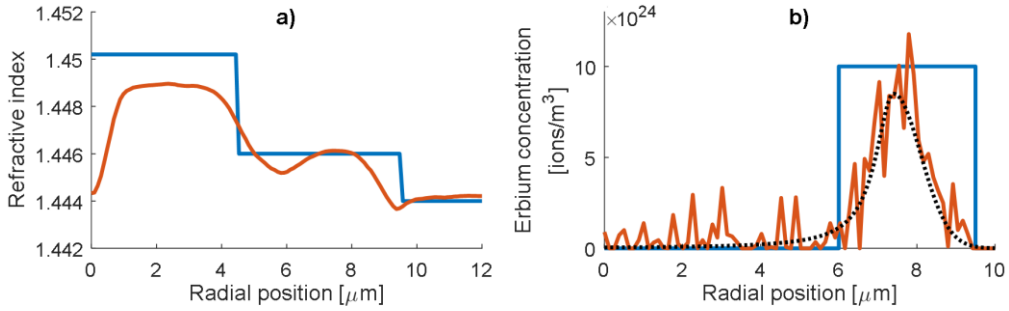

Fig. 5. For the fabricated Fiber B: a) Designed (blue) and measured (orange) refractive index profile. b) Designed (blue), measured (orange), and fitted (black, dotted) erbium concentration profile.

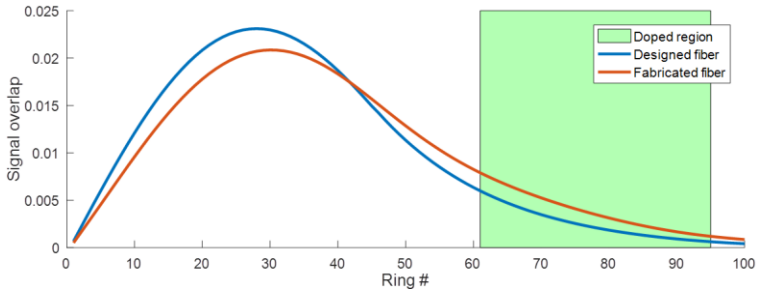

Fig. 6. Signal overlap of each ring in the designed (blue) and fabricated (orange) fiber.

The pump absorption, when injected in the cladding, was measured using the setup and the procedure shown in Fig. 7. The setup consists of an incoherent white-light source followed by a free-space tunable bandpass filter before being injected into a 2.15 m coreless optical fiber. First, a reference measurement is done at the output of the coreless fiber [Fig. 7(a)] to ensure that the power at the output of the coreless fiber is below -40 dBm at each wavelength so that we can assume that the fiber has a very low level of population inversion. The filter has a passband of 1 nm and was tuned with steps of 1 nm from 920 nm to 1020 nm. Afterwards, 9.96 m of the fiber under test (FUT), Fiber B, was added between the coreless fiber and the OSA. The insertion loss in dB/m is determined by dividing the total loss of the FUT by its length. The result is shown on Fig. 8.

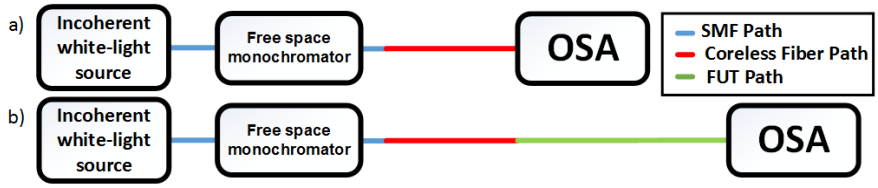

Fig. 7. Characterization setup used to do spectral measurement of the insertion loss when the light is injected in the cladding a) calibration path and b) measurement of the FUT.

To determine background propagation loss, we use the insertion loss values outside the absorption band of Er^{3+} to interpolate the propagation loss value at 980 nm. The background loss was 0.23 dB/m or 0.053 m^{-1}. Such a high background loss can be caused by either impurities at the outer region of the fiber and scattering of pump light out of the fiber. The absorption of the pump is determined by subtracting the background loss (0.23 dB/m) to the absorption in dB/m at 977 nm (0.294 dB/m). The absorption cross-section of the pump is then

National Science and Engineering Research Council of Canada (NSERC) Funding: RDCPJ 515551-17

calculated with Eq. (4), using the pump overlap with the erbium doping, we find σ_{ap}=2.3x10^{-25} m^2.

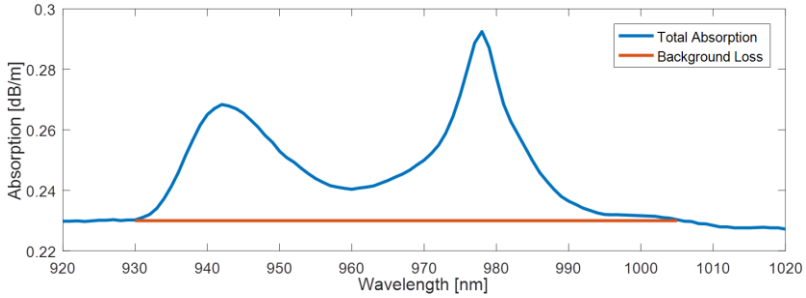

Fig. 8. Spectral measurement of insertion loss when the light is injected in the cladding of the fabricated Fiber B normalized to fiber length.

The absorption and emission cross-sections at the signal wavelengths were determined using a similar setup as shown in Fig. 9. The measurement uses a cut-back technique to determine signal absorption in the fundamental mode. Absorption and emission cross-sections are then calculated from the spectral absorption result. Once again, a wide-band source with a very low output power is used to ensure a negligible level of population inversion. At first, SMFs are spliced at both ends of the 10.00 m FUT with an active alignment procedure. In order to filter higher-order modes, three loops of 2.2 cm of diameter were made after the first splice. Then, the band pass filter was tuned in steps of 1 nm from 1420 nm to 1620 nm. Finally, a length of 7.90 m of the FUT is cut and the two remaining portions of the FUT are spliced back together resulting in a remaining FUT length of 2.1 m in Fig. 9b. This allows to keep the same splices between the SMF and the FUT. The absorption in dB/m is then found by dividing insertion loss difference by 7.90 m. The result is shown in Fig. 10 where it can be observed that the signal propagation background loss is negligible. Also, small oscillations are present on the spectrum, most probably caused by the presence of residual higher-order modes.

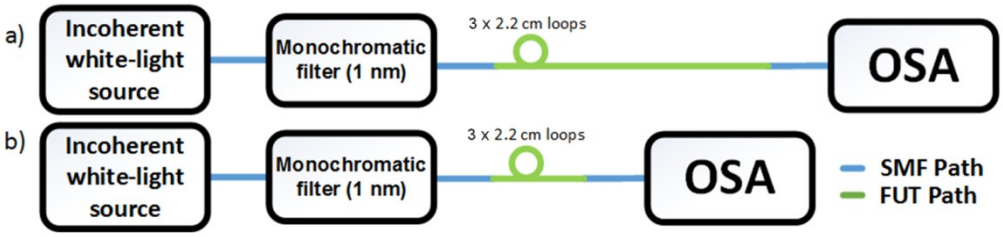

Fig. 9. Characterization setup used to do spectral measurement of the insertion loss when the light is injected in the core a) calibration path and b) measurement of the FUT.

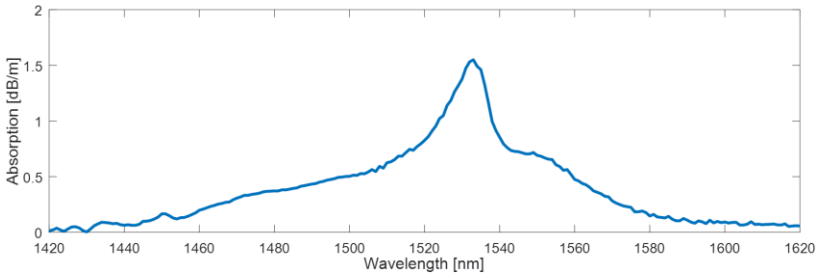

Fig. 10. Absorption spectrum when light is injected in the core of the fabricated Fiber B.

National Science and Engineering Research Council of Canada (NSERC) Funding: RDCPJ 515551-17

Then, considering the experimentally determined signal overlap and Er^{3+} doping concentration in each ring, we use the McCumber relation [29] to determine the absorption and emission cross-sections.

$$\sigma_a(\nu)[m^2] = \frac{\alpha[dB/m]}{(10\,log_{10}e)\sum_i \rho_i[ions/m^3]\Gamma_i} \quad (4)$$

$$\sigma_e(\nu) = \sigma_a(\nu)e^{(\varepsilon - h\nu)/kT} \quad (5)$$

$$\text{where } \varepsilon = \frac{hc}{1535\,nm}$$

The resulting cross-section curves, displayed in Fig. 11, slightly differ from the curves used for the fiber design. The maximum emission occurs at 1533 nm instead of 1532 nm and a shallow hole appears in the emission cross-section spectrum between 1540 nm and 1546 nm. Those differences could be caused by the presence of germanium in the erbium-doped region [30]. Using these cross-sections in the numerical simulations (with all other parameters fixed corresponding to the design values) leads to an optimal fiber length of 19.6 m and a minimum gain of 14.8 dB.

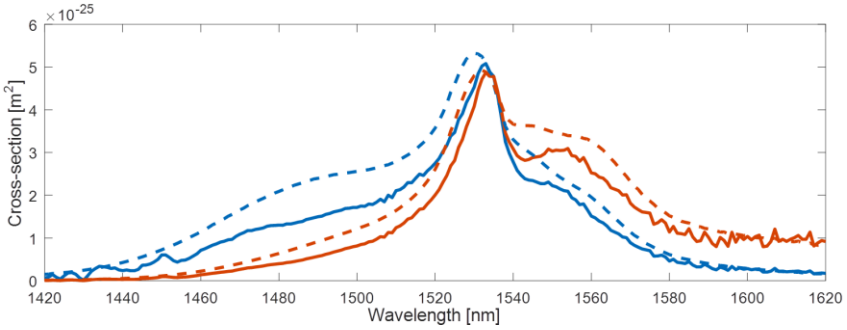

Fig. 11. Absorption (blue) and emission (orange) cross-sections as a function of wavelength when the signal is injected in the core of the fabricated Fiber B (solid) compared with the cross-sections used for the simulations of the designed fiber (dashed).

3.2 Amplifier characterization and validation of the approach

Aiming for a maximum of 4 dB of gain compression when total input signal power varies between -40 dBm and 3 dBm, we used 15 m of the erbium-doped fiber under test (EDFUT), i.e. the fabricated Fiber B with erbium doping in an annular region of the cladding. The gain and noise figure (NF) were measured as a function of wavelength for three different input power values: -40 dBm, -7 dBm and 3 dBm. In the setup shown in Fig. 12, the tunable laser #1 is used as a saturating tone at 1550 nm while the tunable laser #2 is used as a low power tunable wavelength signal (1530 nm – 1560 nm, at least 12 dB weaker than P_{in}). For measurements with P_{in}= -40 dBm, no saturating tone is used. Input and output powers were measured on an OSA at the output of the respective input and output isolators. The 25 W 980-nm pump laser is injected in the cladding of the EDFUT. To achieve the injection, a tapered coreless fiber is spliced at the pigtail of the laser source while its tapered section is rolled around the EDFUT [13]. To filter the remaining pump in the cladding at the output of the fiber, a pump dump, consisting of etching cream applied over 5 cm of the EDFUT, is used. The polarization-dependent effects in the EDF were suppressed by using a polarization scrambler. In order to suppress weakly guided higher-order modes, three fiber loops of 2.2 cm diameter were rolled at 0.5 m and 14.5 m of the EDFUT length as shown on Fig. 12.

National Science and Engineering Research Council of Canada (NSERC) Funding: RDCPJ 515551-17

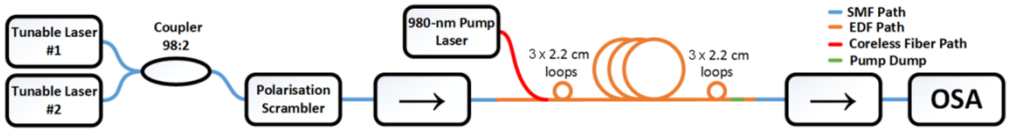

Fig. 12. Setup used to measure the gain and noise figure of the EDF.

Measured and simulated spectral gain and NF are compared in Fig. 13 for the three P_{in} values. The simulations assume that 14.5 W of pump power is coupled in the EDFUT cladding (considering loss in the coreless fiber of 3.6 dB/m this translates into a coupling efficiency of 70%).

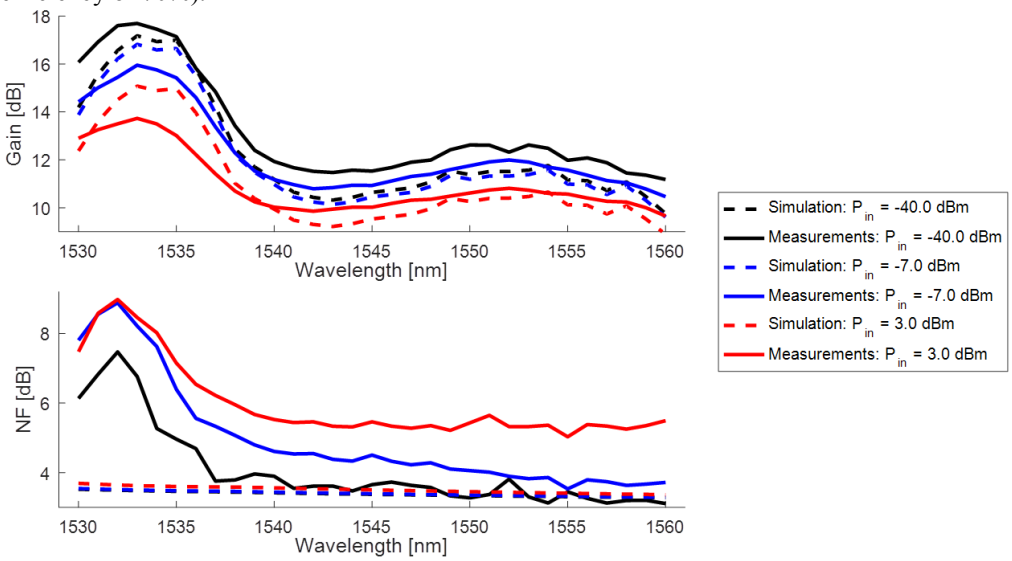

Fig. 13. Gain (top) and NF (bottom), simulations (dashed) and measurements (solid), as a function of wavelength for different total input power.

Simulations and experiments are in good agreement with a maximum gain difference of 2.0 dB. Also, in the experiment, the gain compression when P_{in} changes from -40 dBm to 3 dBm, was 4.1 dB and occurred at 1532 nm in the experiment, while it was 2.1 dB in the simulations and occurred at 1533 nm with the experimentally measured parameter. According to the simulations with all experimentally determined parameters, the gain compression of 4 dB should occur with a fiber length of 19.9 m and lead to a minimum gain of 10.9 dB with P_{in}=3 dBm. Among the factors that could be responsible for this difference between the measured and calculated spectral gain are the presence of residual higher-order modes that are neglected in the model and, also, the fact that the refractive index and erbium doping profiles were measured on a section of the preform but not on the fiber itself. There is a larger difference between the measured and simulated NF, particularly at the shortest wavelengths. Factors that could contribute to this discrepancy include the presence of un-pumped EDFUT sections (before pump coupling and after the pump dump) and the presence of residual higher-order modes, particularly at the shortest wavelengths. Therefore, we believe that the NF peak should be suppressed in future design of annular doped EDF with singlemode core. It should be noted that the 4 dB of gain compression, for total input power variations from -40 dBm to 3 dBm, was achieved with a minimum gain of 9.7 dB. Although this result is very far from the 17.7 dB expected from the design, it is still superior to the simulation results of Fiber A (6.8 dB) and C (8.1 dB). This significant difference can be explained by a thinner erbium-doped region, a significantly higher signal overlap and power intensity in the doped region and differences in cross-sections compared to initial expectations. Higher signal overlap in

National Science and Engineering Research Council of Canada (NSERC) Funding: RDCPJ 515551-17

this annular-doped region means higher signal intensity that will lead to saturation and more gain compression. Nevertheless, the good agreement between measurements and simulations using the experimentally determined parameters indicate that refinement of the fiber fabrication technique should lead to the expected performance. It is also important to note that a flat gain spectrum cannot be achieved with unsaturated amplifiers. Thus, this amplifier with low gain compression is designed to be operated with a gain equalization filter.

4. Conclusion

Through numerical simulations we compared various erbium doping profiles of cladding-pumped single-core fiber amplifiers to maximize its minimum gain while limiting gain compression to less than 4 dB. The results show that inserting the Er^{+3} in an annular region of the cladding near the core leads to better performance. Compared to designs with uniform erbium doping in the core, the proposed design saturates at higher input signal power due to the small overlap of the signal mode with the annular-doped region. A longer erbium-doped fiber length is required but the minimum gain is significantly increased compared to uniform doping in the core. The approach was validated by fabricating and characterizing a single-core double-cladding fiber with erbium doping in an annular region of the cladding. A low gain compression was achieved but the targeted minimum gain could not be demonstrated with this fiber. Nonetheless, the measured minimum gain was still better than the simulated values for erbium-doped fibers with uniform doping in the core. Simulations performed with experimentally determined parameters were compared to measurements showing an agreement within 2 dB for the spectral gain, which gives confidence that performance matching more closely the target will be obtained with improvements in fiber fabrication. Some aspects to be refined include the index profile that will have to be modified to ensure single-mode operation over the whole spectral band and the pump background loss that should be reduced. Our results confirm that this type of design would be of interest for multicore EDFAs with reduced gain variations for different input channel reconfigurations.

Funding

This work is funded by NSERC through a partnership grant with Nokia (RDCPJ 515551-17).

Acknowledgments

The technical help and insights of Mr. Nicolas Grégoire and Mr. Steeve Morency are acknowledged.